



## Optical and physical evaluation of $\text{Al}_2\text{O}_3$ containing strontium phosphate glasses

*D. Shosha<sup>1</sup>, A. M. Abdelghany<sup>2</sup>, M. I. Abdelghany<sup>1</sup>, G. El-Damrawi<sup>1</sup>*

<sup>1</sup> Glass Research Group, Physics Department, Faculty of Science, Mansoura University, 35516, Mansoura, Egypt

<sup>2</sup> Spectroscopy Department, Physics Research Institute, National Research Centre, 33 ElBehouth St., Dokki, 12311, Giza, Egypt

Received:11/10/2022  
Accepted:11/10/2022

**Abstract:** Glasses of nominal composition  $50\text{P}_2\text{O}_5-(49-x)\text{SrO}-1\text{AlF}_3-x\text{Al}_2\text{O}_3$  (mol%) ( $0 \leq x \leq 4.5$ ) were successfully synthesized through melt-quenching route. Synthesized glasses are transparent with amorphous network structure as revealed by x-ray diffraction (XRD). Density measurement reveals minor changes in both density and molar volume associated with the variation of aluminum content and approves the presence of  $\text{AlO}_4$  structural units indicating that aluminum oxide enters partially as a glass former. The optical energy gap calculations of the studied transparent glassy samples containing aluminum oxide reveal minor changes combined with aluminum oxide content. This also can be understood in the shade of the increase in the Al-O-P bonds in parallel with bridging oxygen.

**Keywords:** Strontium phosphate glass; Aluminum oxide; UV/Vis. spectroscopy; X-ray diffraction.

### 1. Introduction

In the past several decades, phosphate glasses have drawn a lot of attention from academics due to their numerous distinctive properties compared to both silicate and borate glasses [1-3]. Phosphate glasses are generally characterized by their low melting temperature and higher coefficient of thermal expansion combined with high transmission in the UV region [3-6]. Due to their distinctive properties, phosphate glasses find several applications in many fields.

The stability of phosphate glasses may be enhanced through the addition of one or more intermediate oxides including  $\text{CaO}$ ,  $\text{CuO}$ ,  $\text{Al}_2\text{O}_3$ , etc. that increase their cross-linking density and increase their chemical durability. It was previously reported that vitreous phosphate glasses are made up of tetrahedral units that are randomly connected by their corners and have three bridging oxygen atoms and one non-bridging oxygen atom apiece [7, 8].

The  $\text{Al}_2\text{O}_3$  may play a dual role as a glass former and modifier to enhance the physical properties of glasses including toughness and hardness that makes the material durable against corrosion [9, 10]. Within the strontium

phosphate glasses, strontium ions act primarily as glass modifiers. The number of non-bridging oxygen (NBO) per tetrahedron on average in the structure of strontium phosphate glasses increases with increasing SrO content. With increasing SrO content, the P=O bonding intensity in the phosphate glasses decreases; O-P-O bonding is diminishing, while  $\text{PO}^-$  bond strength increases. Two main types of strontium sites-modifier and former are documented to be present [8, 11, 12].

The presented work aims to introduce a correlation between the structural changes resulting from aluminum oxide increasing content and their effect on both the mechanical and optical properties of the studied glasses.

### 2. Experimental Work

#### 2.1. Sample preparation

Studied base  $\text{SrO-P}_2\text{O}_5$  glassy samples were synthesized through the traditional melt quenching route. Glassy samples with basic chemical composition  $50\text{P}_2\text{O}_5-(49-x)\text{SrO}-1\text{AlF}_3-x\text{Al}_2\text{O}_3$  (mol%) ( $0 \leq x \leq 4.5$ ) were synthesized using analytical grade chemicals. Table (1) introduce the nomination and composition of each sample. Ammonium

dihydrogen phosphate ( $\text{NH}_4\text{H}_2\text{PO}_4$ ) is the source of  $\text{P}_2\text{O}_5$  and  $\text{SrCO}_3$  as the  $\text{SrO}$  source while  $\text{AlF}_3$  and  $\text{Al}_2\text{O}_3$  were used as received. All chemicals are of high purity > 99% and were supplied by Sigma Aldrich company. Pre-calculated amounts of each raw material were weighed separately and mixed according to molar composition in an agate mortar. The mixture was then placed in a high-temperature furnace regulated at about 350 °C for about 30 min. in a 50 ml porcelain crucible to remove  $\text{NH}_3$ ,  $\text{H}_2\text{O}$ , and carbon dioxide. The temperature of the electric muffle was then raised to 1050–1150°C depending on the glass composition. Homogenization of the melt was achieved by stirring several times at fixed time intervals. Bubble-free melt was poured onto warmed stainless-steel plates with the required dimensions. The sample was then transformed into another oven regulated at about 300°C to remove thermal stresses. The oven was then switched off to cool slowly and samples were stored in a dry place. All samples were observed to be transparent and bubble-free as shown in Figure (1).

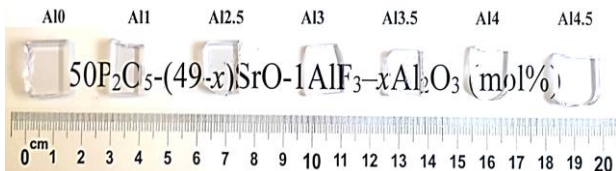


**Fig (1)** studied transparent samples

**Table (1)** Glass nomination and compositions.

Sample	SrO	$\text{P}_2\text{O}_5$	$\text{AlF}_3$	$\text{Al}_2\text{O}_3$
Al0	49.0	50	1	0.0
Al1	48.0	50	1	1.0
Al2.5	46.5	50	1	2.5
Al3	46.0	50	1	3.0
Al3.5	45.5	50	1	3.5
Al4	45.0	50	1	4.0
Al4.5	44.5	50	1	4.5

## 2.2 Sample Characterization

X-Ray diffraction pattern was recorded using a Shimadzu X-ray diffract meter (Model Dx-30) within a Bragg angle extended from 5–70°. The density of the glass samples was assessed using xylene as an immersion solvent. Using Archimedes' method, the glass density ( $\rho_s$ ) was determined at room temperature (30 °C). A bulk solid sample was weighed in the solvent ( $W_{SL}$ ) and air ( $W_{SA}$ ) on a digital scale, and its density was calculated as the mean of the three values using the formula:

$$\rho_s = \frac{W_{SA}}{W_{SA} - W_{SL}} \rho_L \quad (1)$$

Where  $\rho_L$  is the density of xylene.

Molar volume ( $V_m$ ) also calculated in terms of glass density and molecular weight of specific composition (M) using the formula [12, 13]:

$$V_m = M/\rho_s \quad (2)$$

UV–Vis absorption spectra of polished parallel side samples with a constant thickness (2mm±0.1) were immediately measured in the range of 200–1000 nm using a recording double beam spectrophotometer (JASCO 570, Japan) with a spatial resolution of 1 nm.

## 3. Results and Discussion

### 3.1.Density and molar volume

Figure (2) reveals the variation of both density and molar volume of the studied glasses as a function of aluminum oxide concentration.

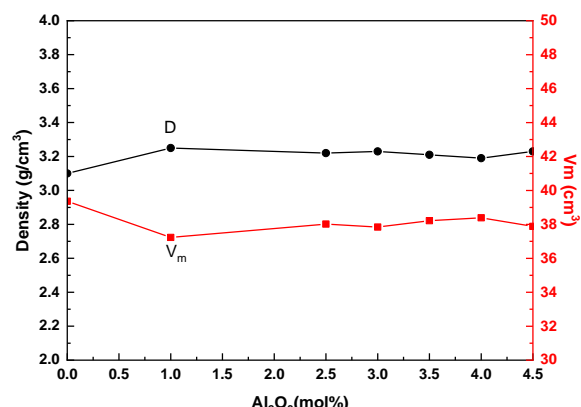


**Fig (2)** the variation of both density and molar volume of the studied glasses as a function of aluminum oxide concentration

The density is observed to be increased with the first addition of 1 mol% of  $\text{Al}_2\text{O}_3$  in the prepared samples (from 3.10 to 3.25  $\text{g}/\text{cm}^3$ ) due to the dual structural role played by  $\text{Al}_2\text{O}_3$  as a glass former and modifier replacing  $\text{SrO}$  modifier. Moreover, the average density of the remaining samples in glass series is around 3.23  $\text{g}/\text{cm}^3$  and nearly constant, this may be related to the molecular weight of  $\text{Al}_2\text{O}_3= 101.96 \text{ g/mol}$  (the density of  $\text{Al}_2\text{O}_3= 3.95 \text{ g}/\text{cm}^3$ ) is in the range of molecular weight of  $\text{SrO}= 103.62 \text{ g/mol}$  in addition to, 101.96  $\text{g}/\text{mol}$  (the density of  $\text{SrO}= 4.7 \text{ g}/\text{cm}^3$ ).

Also, as in figure (2), the behavior of the measured molar volume is the inverse of the density behavior. However, the replacement of

SrO by  $\text{Al}_2\text{O}_3$  leads to increase of the oxygen content in glass network, but most of  $\text{Al}_2\text{O}_3$  would suppress the continued formation of NBO in phosphate network and the molar volume of the formed structural units is nearly constant (around  $37 \text{ cm}^3/\text{mol}$ ) except 0 mol%  $\text{Al}_2\text{O}_3$  (about  $39 \text{ cm}^3/\text{mol}$ ) [14].

### 3.1.XRD analysis

Figure 3 displays the X-ray diffraction patterns for the investigated  $50\text{P}_2\text{O}_5-(49-x)\text{SrO}-1\text{AlF}_3-x\text{Al}_2\text{O}_3$  (mol%) glasses with various  $\text{Al}_2\text{O}_3$  additive concentrations.

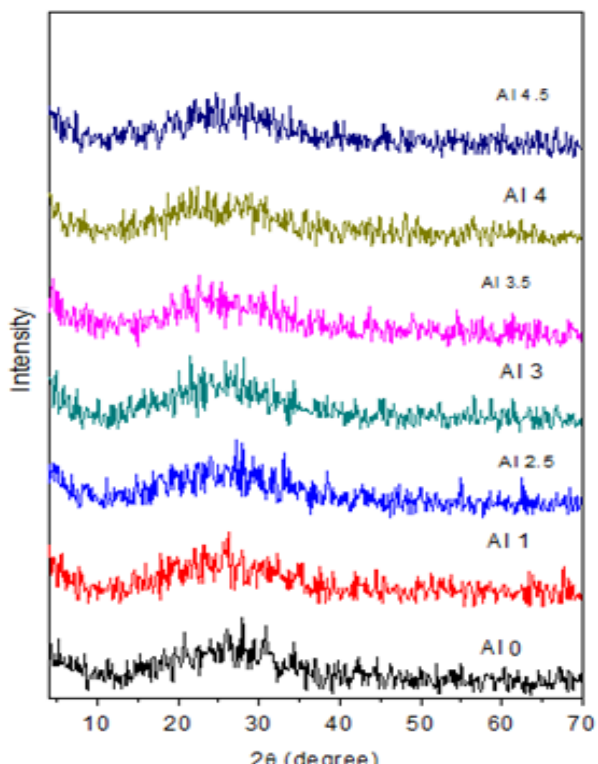


**Fig 3.** XRD patterns of the studied  $\text{Al}_2\text{O}_3$ -Strontium Phosphate glasses

All of the investigated samples show an amorphous behavior supported by the spectral data within the Braggs angle extended from 5-70°. The amorphous phase profiles exhibit only humps lie between 10 to 40 at all concentrations.

### 3.2. UV/Visible optical absorption spectra

UV/Visible optical absorption spectral data or electronic transitions can be considered a quantitative technique that is used to measure how much a chemical substance absorbs light. This is accomplished by comparing the amount of light that passes through a sample to the amount of light that goes through a reference sample or a blank.

Figure (4) reveals the optical absorption spectral data of the studied glasses containing variable amounts of aluminum oxide. Obtained spectra reveal nearly the same behavior consisting of a strong absorption band located at about 230-250 nm within the Uv range with a sharp absorption edge exactly after such a strong band. The absorption edge was also found to be shifted towards a shorter wavelength that can be correlated to the corresponding optical energy gap or transparency of the studied sample as a function of aluminum oxide content and without any other absorption band in the visible range till the end of measurements.

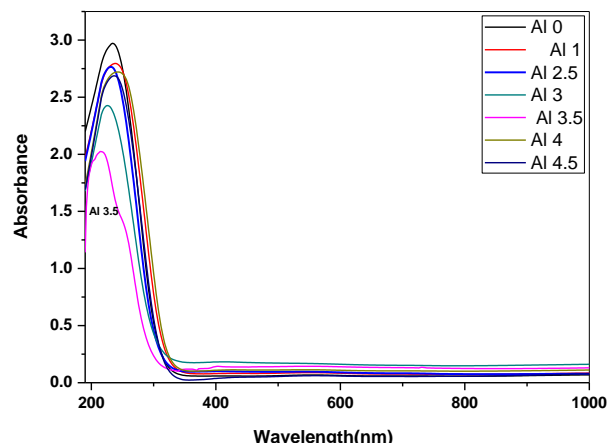


**Fig (4)** UV-Vis absorption spectra of the studied glasses.

The absorption of UV or visible radiation corresponds to the excitation of outer electrons utilizing transition involving charge-transfer electrons and/or transitions of d and f electrons. Vibrations and rotations in such cases also have discrete energy levels, which can be considered as being packed on top of each electronic level.

The behavior of an electron in solids is related to the behavior of the network or compartment and the role of each component in combination with their concentration of all constituents in the glassy matrix [15, 16].

A specific crystal momentum ( $k$ -vector) in the Brillouin zone distinguishes the minimal-energy state in the conduction band from the maximal-energy state in the valence band. The material has an "indirect gap" if the  $k$ -vectors are different. If the crystal momentum of electrons and holes in the conduction band and the valence band are the same, the band gap is said to be "direct," and an electron can then emit a photon directly. Since the electron must

pass through an intermediate state and transmit momentum to the crystal lattice, a photon cannot be released in an "indirect" gap [15].

The optical absorption process produced by electronic transitions can provide quick information about the band structure and energy gap of crystalline and amorphous materials. We determined the band gap values for an indirect and direct allowed transition of all investigated samples using the Mott and Davis [15-18] formula:

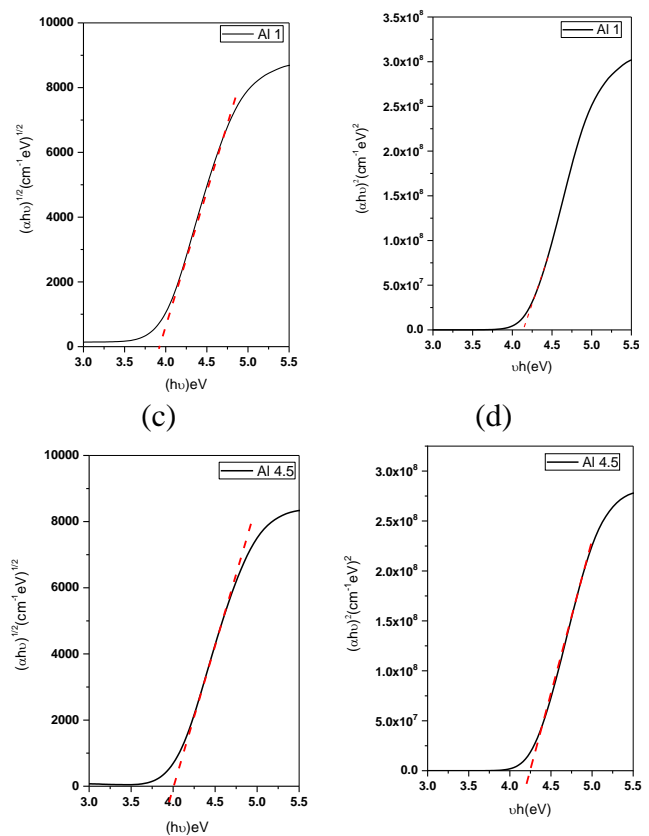
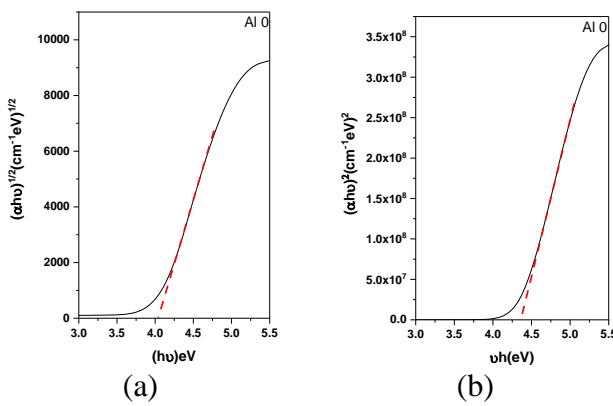
$$\alpha h\nu = B(h\nu - E_g)^r \quad (2)$$

where B: a constant,  $\alpha$  the absorption coefficient,  $E_{\text{opt}}$ : the optical band gap energy,  $h$  is plank constant.

For indirect allowed transition,  $(\alpha h\nu)^{0.5}$  versus  $(h\nu)$ , while for direct allowed transition the  $(\alpha h\nu)^2$  is plotted against  $(h\nu)$ . Figure (5, a:f) shows exemplified Tauc plots for the energy gap values of direct and an indirect allowed transition of base glass and samples containing 1 and 4.5 Aluminium oxide respectively; these results are listed in Table (2). The energy gap values are decreased with increasing aluminum oxide content combined with the increase in the non-bridging oxygen bonds [19, 20].

Figure (6. a, b, c) reveals the variation of both direct and indirect energy gaps with the change in aluminum oxide content.

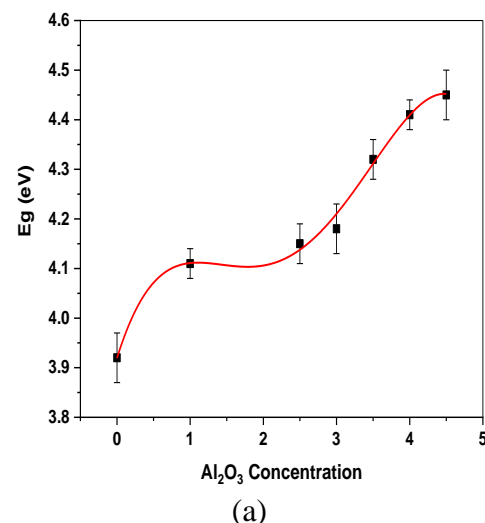
It was clear that the presence of both  $P_2O_5$  and  $AlO_4$  as a mixed glass former network species enhances the optical, mechanical strength, and other physical characteristics of the glass that is modified with  $SrO$  modifier. This also can be understood in the shade of the increase in the Al-O-P bonds in parallel with bridging oxygen.



**Fig (5)** Tauc plots of base glass and samples containing 1 and 4.5 Aluminium oxide

**Table (2)** estimated energy gap of the studied samples

Sample	Eg	Eg indirect (eV)	Eg direct (eV)
Al0	4.11	4.038	4.35
Al1	3.92	3.93	4.18
Al2.5	4.08	4.05	4.34
Al3	4.18	4.12	4.38
Al3.5	4.32	4.24	4.74
Al4	3.89	3.85	4.12
Al4.5	4.01	4	4.27



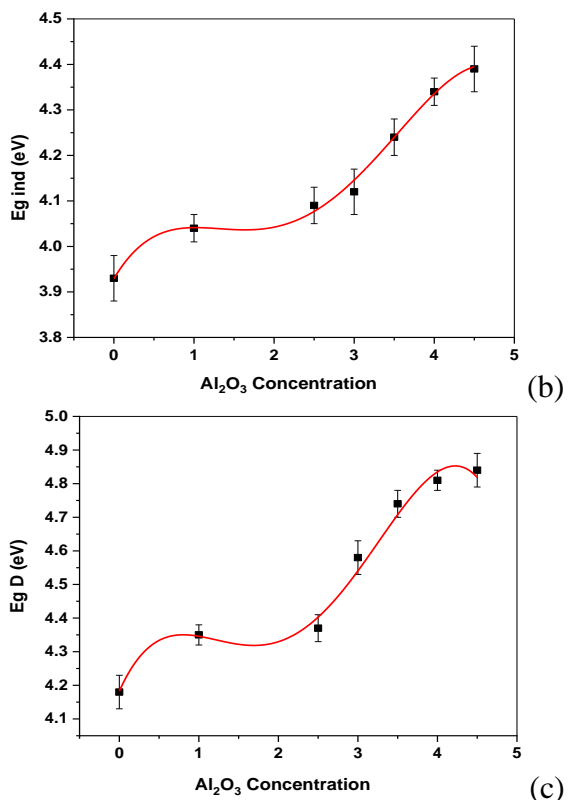


**Fig (6. a, b, c)** variation of both direct and indirect energy gaps with the change in aluminum oxide content.

#### 4. Conclusions

Studied glasses of composition [50P<sub>2</sub>O<sub>5</sub>-(49-x)SrO-1AlF<sub>3</sub>-xAl<sub>2</sub>O<sub>3</sub> (mol%) ( $0 \leq x \leq 4.5$ )] were synthesized by melt-quenching technique. transparent glass samples approved to be amorphous as revealed by x-ray diffraction (XRD). Density and molar volume measurement reveals minor changes associated with the variation of aluminum oxide content and approves the formation of AlO<sub>4</sub> structural units indicating that aluminum oxide enters glassy matrix partially as a glass former. The optical energy gap calculations of the studied transparent glassy samples containing aluminum oxide reveal minor changes coorelated with the minor additions of aluminum oxide content. This also can be understood in the shade of the increase in the Al-O-P bonds in parallel with bridging oxygen.

#### References

1. Brow, R. K. (2000). The structure of simple phosphate glasses. *Journal of Non-Crystalline Solids*, **263**, 1-28.
2. Eraiah, B., & Bhat, S. G. (2007). Optical properties of samarium doped zinc-phosphate glasses. *Journal of Physics and Chemistry of Solids*, **68(4)**, 581-585.
3. Brauer, D. S. (2012). Phosphate glasses. Bio-glasses: an introduction, 45-64.
4. Sharmin, N., & Rudd, C. D. (2017). Structure, thermal properties, dissolution behaviour and biomedical applications of phosphate glasses and fibres: a review. *Journal of Materials Science*, **52(15)**, 8733-8760.
5. Pascuta, P., Bosca, M., Borodi, G., & Culea, E. (2011). Thermal, structural and magnetic properties of some zinc phosphate glasses doped with manganese ions. *Journal of Alloys and Compounds*, **509(11)**, 4314-4319.
6. Shaaban, K. S., Al-Baradi, A. M., & Ali, A. M. (2022). Physical, optical, and advanced radiation absorption characteristics of cadmium lead phosphate glasses containing MoO<sub>3</sub>. *Journal of Materials Science: Materials in Electronics*, **33(6)**, 3297-3305.
7. Mountjoy, G. (2022). Phosphate Glasses. Atomistic Simulations of Glasses: Fundamentals and Applications, 295-346.
8. Abdelghany, A. M., El-Damrawi, G., Oraby, A. H., & Madshal, M. A. (2018). Optical and FTIR structural studies on CoO-doped strontium phosphate glasses. *Journal of Non-Crystalline Solids*, **499**, 153-158.
9. Stoch, P., Goj, P., Wajda, A., & Stoch, A. (2021). Alternative insight into aluminium-phosphate glass network from ab initio molecular dynamics simulations. *Ceramics International*, **47(2)**, 1891-1902.
10. Möncke, D., & Eckert, H. (2019). Review on the structural analysis of fluoride-phosphate and fluoro-phosphate glasses. *Journal of Non-Crystalline Solids: X*, **3**, 100026.
11. El Jouad, M., Touhtouh, S., Sadek, O., & Hajjaji, A. (2022). Structural studies on varied concentrations of europium doped strontium phosphate glasses. *Materials Today: Proceedings*.
12. Chanshetti, U. B., Shelke, V. A., Jadhav, S. M., Shankarwar, S. G., Chondhekar, T. K., Shankarwar, A. G., ... & Jogad, M. S.

- (2011). Density and molar volume studies of phosphate glasses. *Facta universitatis-series: Physics, Chemistry and Technology*, **9(1)**, 29-36.
13. Shaalan, M., El-Damrawi, G., Hassan, A., & Misbah, M. H. (2021). Structural role of Nd<sub>2</sub>O<sub>3</sub> as a dopant material in modified borate glasses and glass ceramics. *Journal of Materials Science: Materials in Electronics*, **32(9)**, 12348-12357.
  14. Ahmed, M. R., Sekhar, K. C., Ahammed, S., Sathe, V., Alrowaili, Z. A., Amami, M., & Shareefuddin, M. (2022). Synthesis, physical, optical, structural and radiation shielding characterization of borate glasses: a focus on the role of SrO/Al<sub>2</sub>O<sub>3</sub> substitution. *Ceramics International*, **48(2)**, 2124-2137.
  15. Bouabdalli, E. M., Jouad, M. E., Hajjaji, A., & Touhtouh, S. (2022). First investigation of the effect of strontium oxide on the structure of phosphate glasses using molecular dynamics simulations.
  16. Mott, N. F. (1972). Conduction in non-crystalline systems IX. the minimum metallic conductivity. *Philosophical Magazine*, **26(4)**, 1015-1026.
  17. Mott, N. F., & Davis, E. A. (2012). Electronic processes in non-crystalline materials. Oxford university press.
  18. Ikramov, R. G., Mamaxanov, A. A., Nuriddinova, M. A., Jalolov, R. M., Muminov, K. A., & Sultonov, B. Q. (2021). Calculation of the interband absorption spectra of amorphous semiconductors using the Kubo-Greenwood formula. *Journal of Applied Science and Engineering*, **25(5)**, 767-772.
  19. Misbah, M. H., Abdelghany, A. M., El-Agawany, F. I., Rammah, Y. S., & El-Mallawany, R. (2021). On Y<sub>2</sub>O<sub>3</sub>· Li<sub>2</sub>O· Al<sub>2</sub>O<sub>3</sub>· B<sub>2</sub>O<sub>3</sub> glasses: synthesis, structure, physical, optical characteristics and gamma-ray shielding behavior. *Journal of Materials Science: Materials in Electronics*, **32(12)**, 16242-16254.
  20. Misbah, M. H., Abdelghany, A. M., El-Kemary, M., & Rammah, Y. S. (2021). Mixed modifier effect in lithium manganese metaphosphate glasses on the emission of highly dispersed Mn<sup>2+</sup> centers for red-LED. *Ceramics International*, **47(22)**, 32424-32432.